# Research on Hypersonic Inlet Leading Edge Radius Effect on Wall Static Pressure and Heat Flux

*WANG Zhen-feng*, BAI Han-chen*, ZHANG Kou-li***
**Science and Technology on Scramjet Laboratory,Hypervelocity Aerodynamics Institute of CARDC*
*Mianyang, Sichuan 621000,China*
***Hypervelocity Aerodynamics Institute of CARDC*
*Mianyang Sichuan 621000, China*

## Abstract
The effect of two-dimensional hypersonic inlet leading edge radius(*SR*) on wall static pressure and heat flux on three external compression surfaces was studied by experimentation and CFD. The length of test models is 0.6 meter, and range of *SR* is 0～3mm. The experiment is executed in shock tunnel at M5.98. It shows that wall static pressure increases gradually reaching a platform on the compression surfaces, while heat flux increases reaching local maximum and then decreases. With *SR* increasing, the pressure platform and heat flux maximum decreases, and the distance reaching pressure platform and heat flux maximum becomes longer.

## 1. Introduction

Considering the thermal protection and technics design, the leading edge of the hypersonic aerocraft must be blunted properly. The flow field character of sharp and blunt leading edge may differ remarkably, and the performance of components and aerocraft may be influenced, therefore the effection and flow field character of blunted leading edge have been studied for long time.

The leading edge to be blunted is an efficient way to reduce heat flux, but it also influence lift[1,2], drag, pitching moment[3] and lift-to-drag ratios character[4], so lots of researcher have studied the ramp/cone leading edge effection for the aerocraft design and aerodynamics and aerothermal performance evaluation.

The 3D numerical results of CAO De-yi[4] indicate that the blunted leading edge has limited effect on the lift of the vehicle, but has great influences on the drag and lift-to-drag ratio. CFD is used by LIU Ji-min to analyze the influence of blunt leading edge on the performance of waverider[1] and performance in off-design regimes[5], the results show that performances of lift-to-drag ratios of waveriders and max heat fluxes are affected not only by blunt radius,but also by the blunted method, and the variation laws of aerodynamic coefficients in off-design regimes are almost the same. Different blunt radius' influence to waverider's aero force and aero heat performance is studied by CHEN Xiao-qing[2] using fluid dynamics tool, and the results show that blunt leading edge could reduce the maximum heat flux effectively, but it also reduced the aerodynamic performance. Lewis researched the effection of waverider leading edge by experimentation[6] and CFD[7], the results reveal lift-to-drag ratios and drag coefficient from CFD showing good agreement with experiment results, and blunt radius has great influence on the aerodynamic performance.

It is known that compression surfaces of the inlet and forbody of the aerocraft are designed holistically, when the performance of the aerocraft is influenced by the leading edge radius, the shock wave structure on the outer compression surfaces[8], boundary layer thickness and translation state[9,10] is also effected, and so the performance of the inlet. The change of the shock wave structure will influence the static pressure distribution[11]; the boundary layer may influence the available figure of the inlet[12,13], and then the total pressure coefficient and mass flow coefficient; and boundary layer translation state may influence isolator entrance boundary layer resistance separation performance and inlet start-up character. So it is very important to study the effection of leading edge radius for the inlet design.

SHEN Qing and ZHANG Hong-jun found that the inlet with sharp leading edge could start up, while the inlet with blunted leading edge could not start up[14], and the reason is that boundary layer translation position prolongs when leading edge is blunted, and boundary layer resistance separation performance decreases, and separation region extends. The research of WANG Xiao-dong[8] shows that the shock wave structure can be destroyed, and mass flow coefficient decreases, with the radius of forebody leading edge increasing. Zhou Zhong-ping[15] studied the effects of

bluntness on the static pressure distribution of hypersonic inlet and ramp, it shows the static pressure increases on the single stage ramp, but the static pressure on the multilevel compression surfaces inlet is not analyzed detailedly. The published papers show that lots of research work uses CFD, while experimental results is relatively scarce; trend and qualitative conclusion is useful, but quantitive conclusion is scarce. In order to get some quantitive experimental datum, the effect of two-dimensional hypersonic inlet forebody leading edge radius on external compression surfaces flow field is studied by experimentation and CFD, and wall static pressure and heat flux distribution is provided in this paper.

## 2. Research method and testing techniques

### 2.1 Testing model

The testing models which are the external surfaces of hypersonic inlet have three compression surfaces (see Fig. 1), and the flow deflexion angles are 6.06°, 6.98° and 8.09° respectively. The radius of forebody leading edge (*SR*) of models is 0mm (named sharp leading edge model), 0.5mm, 1mm, 1.5mm and 3mm. The first compression surface is tangent to the circle of the leading edge. The length of the sharp leading edge model is about 0.6m, and the width of the model is 0.2m; with the radius of forebody leading edge increasing, the length of the first compression surface shortens, and the other two compression surfaces have same length with the sharp leading edge model.

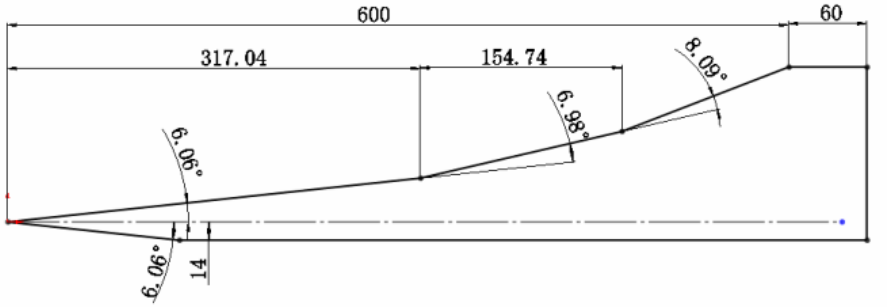


Fig.1 Sketch of testing model, *SR*=0mm

### 2.2 Testing wind tunnel and techniques

The experiment is carried out in 0.6m Shock Tunnel (diameter of nozzle exit is 0.6m) in Hypervelocity Aerodynamics Institute of CARDC; the testing medium is nitrogen, and the testing time is 4ms. The free stream Mach number is 5.98, the total temperature is 670K, the total pressure is 6.557MPa, and Re is $3.37\times10^7$/m. The angle of attacking and yawing are both zero.

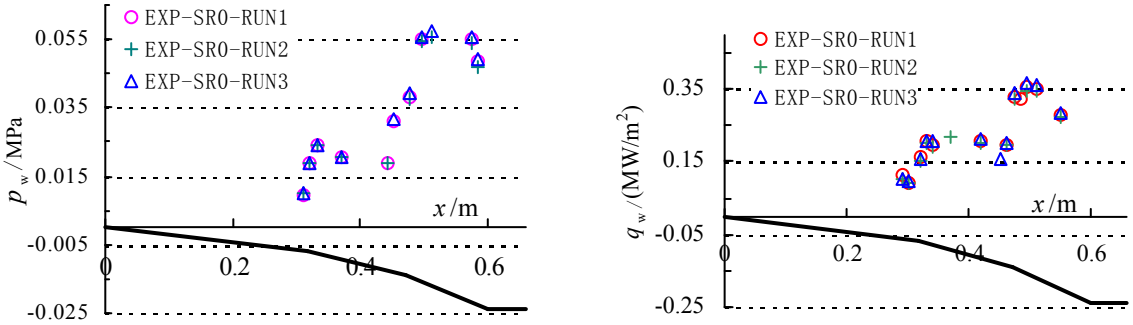


(a) Wall static pressure (b) Wall heat flux

Fig.2 Wall static pressure and heat flux distribution from three runs

The heat flux is measured by platinum thin film resistance thermometer which is one classical method used in shock wave tunnel, with repeatability error less than 8%. The wall pressure is measured by press-resistance sensor, with repeatability error less than 5%. The testing datum of sharp leading edge model from three runs are shown in Fig. 2, in which "EXP" represents experimental result, and it reveal the repeatability of heat flux and static pressure is very good.

### 2.3 CFD method introduction

In order to get more information about the flow field and compare with the experimental datum, two dimensional numerical simulation works is done through Fluent. The static pressure and heat flux datum gotten through three viscous models are compared with experimental datum, including standard *k-ε* model, standard *k-ω* model, and SST *k-ω* model, with near-wall treatment chosen standard wall functions, and spatial discretization chosen two order upwind. The income flow parameters are the same as the wind tunnel calibrating parameters, and the wall static temperature is assumed 300K. The grids near wall and corner are thickened, and the total grids number is about 330 thousand.

## 3. Results

### 3.1 Comparing analyse of wall pressure and heat flux from three different viscous models

Wall pressure and heat flux distribution from three different viscous models and experimentation is shown in Fig. 3 and Fig. 4, in which "KE-STAND", "KW-STAND", and "KW-SST" represents standard *k-ε*, standard *k-ω*, and SST *k-ω* viscous models results, and "SR" represents radius of forebody leading edge.

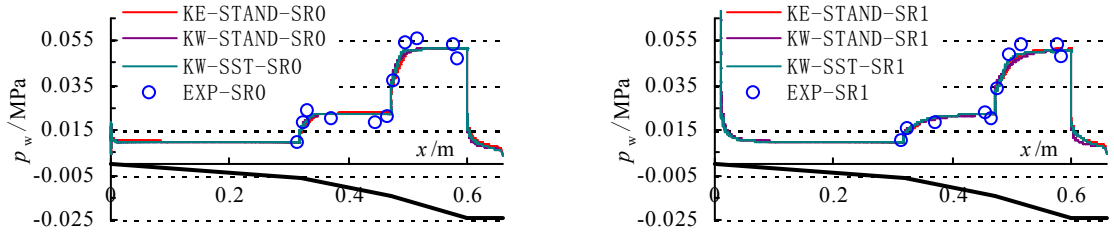


(a) SR=0mm (b) SR=1.0mm

Fig.3 Wall static pressure by three different viscous models

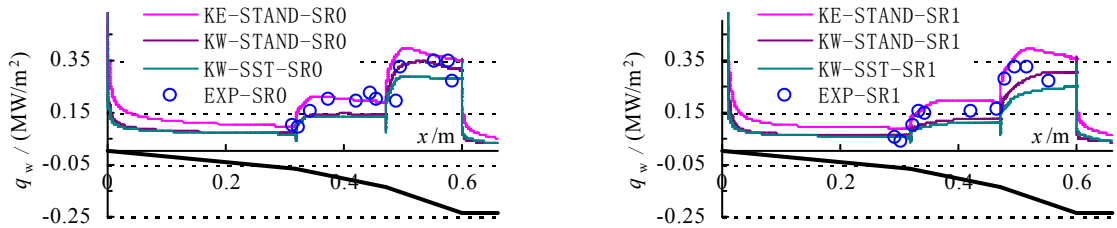


(a) SR=0mm (b) SR=1.0mm

Fig.4 Wall heat flux by three different viscous models

It can be seen in Fig. 3 that wall static pressure from three different viscous models only has little difference near the corners. The wall pressure datum gotten from experiment and CFD is consistent very well; upward the second corner, the experimental result is some lower; downward the second corner, the experimental result is higher about 8%.

It can be seen in Fig. 4 that heat flux from three different viscous models has great difference; the result from standard *k-ε* viscous model is the highest, then the result from standard *k-ω* viscous model, and the result from SST *k-ω* viscous model is the lowest. With the radius of forebody leading edge increasing, the difference of the result from different viscous models increases.

When *SR* is 0mm, the heat flux datum gotten from standard *k-ω* and SST *k-ω* viscous model have little difference on the first and second compression surface, and result from SST *k-ω* viscous model is lower about 30% than that from standard *k-ε* viscous model. Near the heat flux maximum on the third compression surface, the result from standard *k-ω* viscous model is lower about 15%, and the result from SST *k-ω* viscous model is lower about 25%, compared with standard *k-ε* viscous model result. On the second compression surface, the result from standard *k-ε* viscous model and experimental is consistent very well; on the third compression surface, all CFD result has some difference with experimental result, and the result from standard *k-ε* viscous model has minimal difference with experimental result.

When *SR* is 1mm, the heat flux datum gotten from standard *k-ω* and SST *k-ω* viscous model also have little difference on the first and second compression surface; Compared with standard *k-ε* viscous model result, the result from standard *k-ω* viscous model is lower about 35%, and the result from SST *k-ω* viscous model is lower about 40%. On the third compression surface, there is one heat flux maximum for the result from standard *k-ε* viscous model, while no such maximum exists for the result from other two viscous models; based on the heat flux maximum, at the same point, the result from standard *k-ω* viscous model is lower about 25%, and the result from SST *k-ω* viscous model is lower about 40%. On the second compression surface and forepart of the third compression surface, the result from standard *k-ε* viscous model has minimal difference with experimental result.
Generally speaking, the wall pressure datum gotten from experiment and CFD is consistent very well. The heat flux datum gotten from standard *k-ε* viscous model has minimal difference with experimental result.

### 3.2 Wall static pressure distribution for different radius of forebody leading edge models

Wall static pressure distribution from experiment and CFD for different radius of forebody leading edge models is shown in Fig. 5, with standard *k-ε* viscous model chosen. These datum show that wall pressure distribution gotten from experiment and CFD is consistent very well; and on the forepart of the third compression surface, the CFD result is some lower.

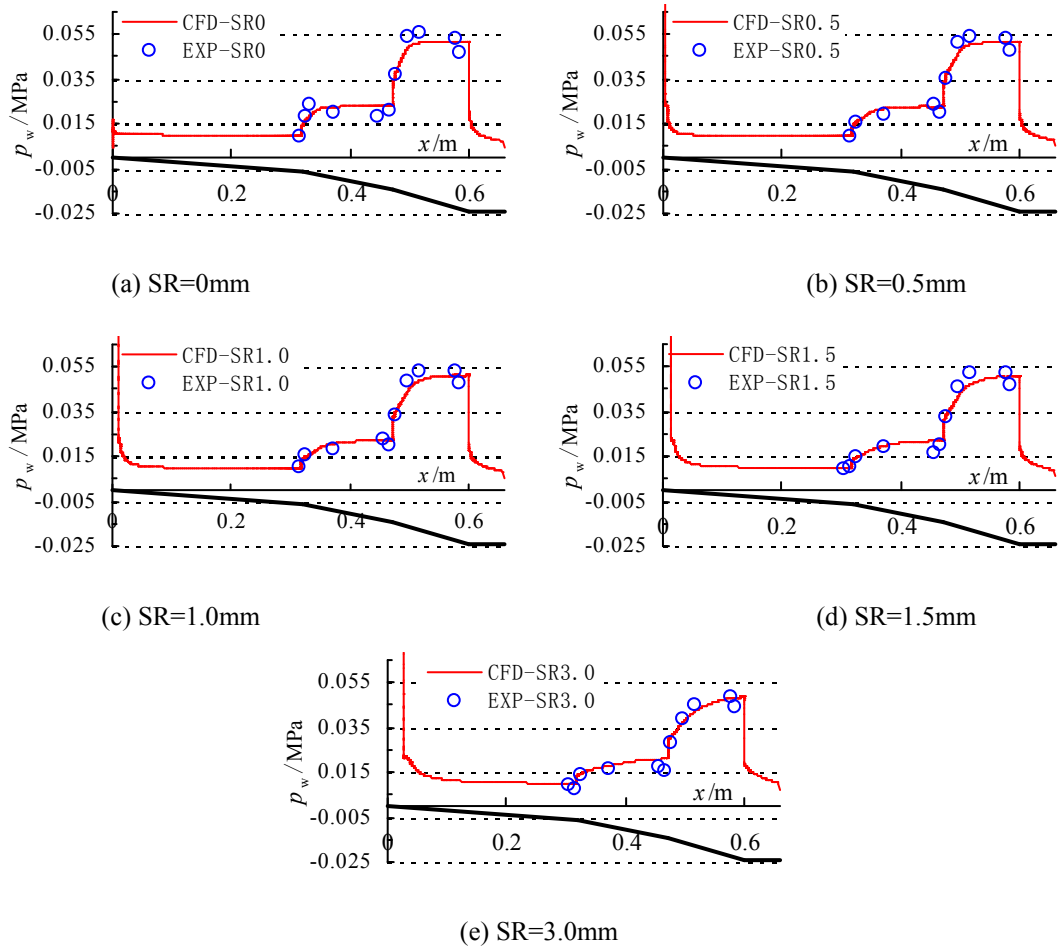


(a) SR=0mm (b) SR=0.5mm

(c) SR=1.0mm (d) SR=1.5mm

(e) SR=3.0mm

Fig.5 Wall static pressure distribution comparison of CFD and experiment

Wall static pressure distribution varying with different radius of forebody leading edge is shown in Fig. 6. The datum from experiment and CFD both show that the varying trend are similar for different radius of forebody leading edge models. Near the forebody leading edge, there is one peak pressure induced by the first shock wave, and this peak pressure is far higher than other pressure value; and then the pressure decreases gradually to one platform on the first compression surface. On the second and third compression surface, the wall pressure increases monotonously induced by shock wave boundary layer interaction. The wall pressure reaches a pressure platform on the second compression surface; on the third compression surface, the wall pressure also reaches a pressure platform when the

radius of forebody leading edge is small, while it increases monotonously when the radius of forebody leading edge is 3mm. Finally, near the shoulder of the testing model, the wall pressure decreases first rapidly and then slowly.

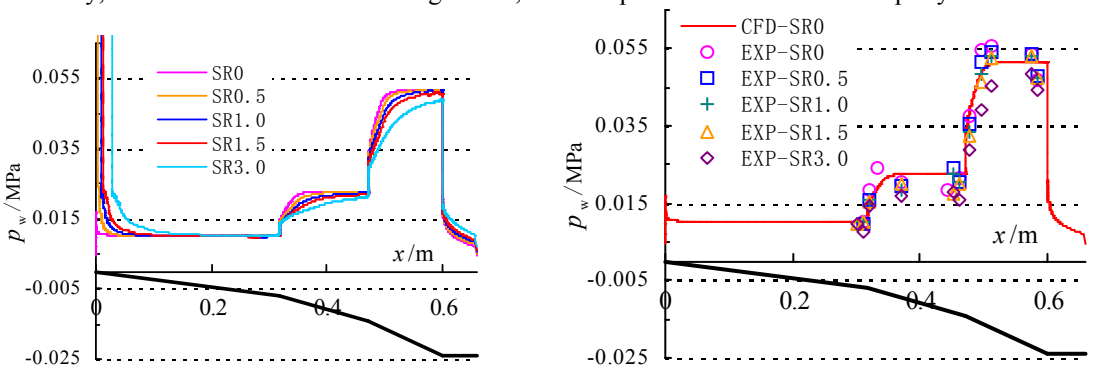


(a) CFD result (b) Experiment result

Fig.6 Wall static pressure distribution varying with *SR*

It also can be seen in Fig. 6 that with the radius of forebody leading edge increasing, wall pressure decreases wholly, the pressure platform also decreases, and the length reaching pressure platform prolongs. At x=0.51m, with *SR* increasing from 0mm to 3mm, the static pressure decrease about 20%. The wall pressure variety induced by the forebody leading edge can change the lift force and static pressure ratio, and then change the lift to drag ratio and inlet start-up character.

### 3.3 Wall heat flux distribution for different radius of forebody leading edge models

Wall heat flux distribution from experiment and CFD for different radius of forebody leading edge model is shown in Fig. 7, and wall heat flux distribution varying with different radius of forebody leading edge is shown in Fig. 8.

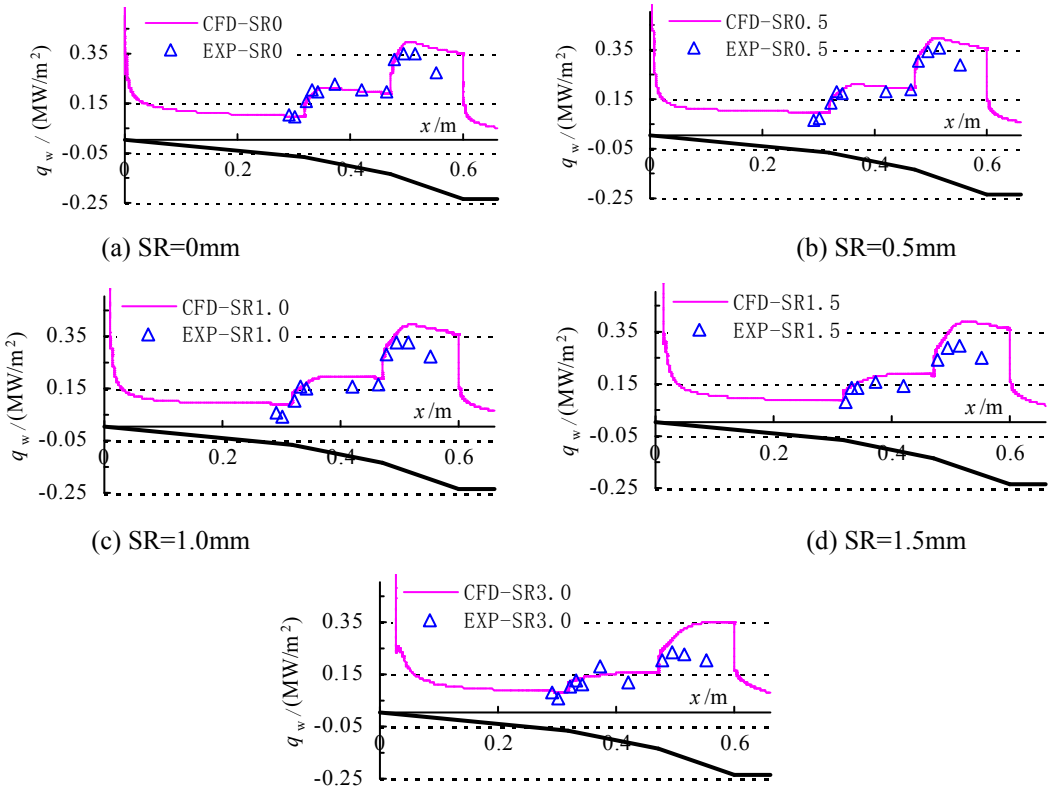


(a) SR=0mm (b) SR=0.5mm

(c) SR=1.0mm (d) SR=1.5mm

(e) SR=3.0mm

Fig.7 Wall heat flux distribution comparison of CFD and experiment

It shows that heat flux datum gotten from experiment and CFD is consistent very well on the front segment of the sharp leading edge model; on the third compression surface, heat flux datum gotten from CFD is higher distinctly than that from experiment, and may higher than about 100% at local position.

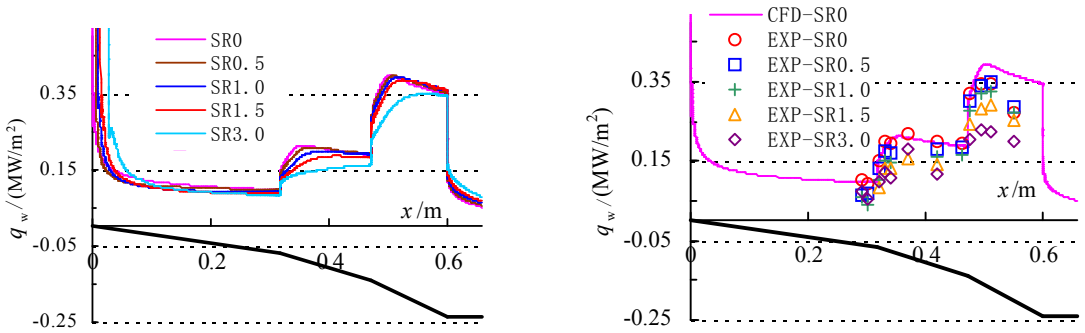


(a) CFD result (b) Experiment result

Fig.8 Wall heat flux distribution varying with *SR*

It is shown in Fig. 8 that there is a low velocity and high heat flux region induced by separated shock wave, and there is a peak heat flux which is far higher than other heat flux value; and then the heat flux decreases gradually on the first compression surface. On the second compression surface, the wall heat flux increases to a local maximum for static temperature increasing and boundary layer thickness decreasing, and then decreases gradually on the compression surface as the boundary layer thickness increasing gradually and heat exchange smothered, and there is not a platform as the static pressure distribution. On the third compression surface, the wall heat flux also reaches local maximum and then decrease gradually when the radius of forebody leading edge is small, while it increases monotonously when the radius of forebody leading edge is 3mm. Finally, near the shoulder of the testing model, the wall heat flux decrease first rapidly and then slowly.

The results from experiment and CFD both show that with the radius of forebody leading edge increasing, wall heat flux decreases wholly; the heat flux local maximum also decreases, and the length reaching heat flux local maximum prolongs. At x=0.51m, with *SR* increasing from 0mm to 3mm, the heat flux decrease about 33% and 18% for experiment and CFD result respectively.

The heat flux variety induced by the forebody leading edge may change the boundary layer translation state and position, and then change the back-pressure resistance and start-up character of the inlet, and influence the design of structure/heat defence of the aerocraft.

## 4. Conclusions

The effect of hypersonic inlet leading edge radius on wall static pressure and heat flux is studied by experiment and CFD, The conclusions of this paper are:

1. The wall pressure varying trend of the testing model with different radius of forebody leading edge is similar: near the forebody leading edge, there is one peak pressure, and then the pressure decreases gradually on the first compression surface; on the second and third compression surface, the wall pressure reaches a pressure platform when the radius of forebody leading edge is small, while it increases monotonously when the radius of forebody leading edge is 3mm; with the radius of forebody leading edge increasing, wall pressure decreases wholly, the pressure platform also decreases, and the length reaching pressure platform prolongs.
2. On the second and third compression surface, the wall heat flux reaches local maximum and then decrease gradually when the radius of forebody leading edge is small; with the radius of forebody leading edge increasing, wall heat flux decreases wholly; the heat flux local maximum also decreases, and the length reaching heat flux local maximum prolongs.
3. Generally speaking, the wall pressure datum gotten from experiment and CFD (using three different viscous models) is consistent very well. The heat flux datum gotten from standard *k-ε* viscous model has minimal difference with experimental result

With the forebody leading edge radius varying, the wall pressure and heat flux distribution changes, the lift to drag ratio of aerocraft and boundary layer translation state varies, and then back-pressure resistance and inlet start-up character may be changed, and then influence the design of structure/heat defence of the aerocraft, so these problems is very important and should be researched in the future.

## References


[1] LIU Ji-min, HOU Zhi-qiang, SONG Gui-bao. Blunted method for waverider and its effect on performance. *Journal of Astronautics*, 2011, 32(5):966-74.

[2] CHEN Xiao-qing, HOU Zhong-xi, LIU Jian-xia. The blunt leading edge's influence to the performance of waverider. *Journal of Astronautics*, 2009, 30(4):1334-1339.

[3] Drayna T W, Nompelis I, Graham V C. Numerical simulation of the AEDC waverider at Mach 8. *AIAA* 2006-2816.

[4] CAO De-yi, LI Chun-xuan. A numerical study on aerothermodynamic performances of a waverider based vehicle. *Journal of Astronautics*, 2008, 29(6):1782-1785.

[5] LIU Ji-min, HOU Zhi-qiang, SONG Gui-bao. Performance analysis of waverider with blunt leading edge in off-design regimes. *FLIGHT DYNAMICS*, 2011, 29(1):21-25.

[6] Gillum M J,Lewis M J. Analysis of experimental results on a mach 14 waverider with blunt leading edges. *AIAA* 96-0812.

[7] Takashima N,Lewis M J. Navier-stokes computation of a viscous optimized waverider. *AIAA* 92-0305.

[8] WANG Xiao-dong, LE Jia-ling. Numerical simulation of effects of leading edge on the performance of inlet. *Journal of Propulsion Technology*, 2002, 23(6):460-462.

[9] PAN Hong-lu, MA Han-dong, WANG Qiang. Large eddy simulation of transition in a hypersonic blunt-wedge boundary layer. *Acta Aeronautica Et Astronautica Sinica*, 2007, 28(2):21-25.

[10] Lau K Y. Hypersonic boundary layer transition–application to high speed vehicle design. *AIAA* 2007-0310.

[11] O'Brien T F, Colville J R. Blunt leading edge effects on inviscid truncated busemann inlet performance. *AIAA* 2007-5411.

[12] Guan Qian-lie, Xing Jun-bo. Study on boundary layer of hypersonic inlets. *Journal of Propulsion Technology*, 1989, (4):19-24.

[13] DONG Hao, WANG Cheng-peng, CHENG Ke-ming. Effect of design parameters and boundary layer correction on performance of jaws inlet. *Journal of Propulsion Technology,* 2010, 31(3):265-269.

[14] ZHANG Hong-jun, YUAN Xiang-jiang, SHEN Qing. Analysis on boundary layer flow stability hypersonic wedge. *Journal of Propulsion Technology*, 2012, 33(5):671-675.

[15] Zhou Zhong-ping. Effects of bluntness on the performance of a hypersonic inlet. MaD Thesis. Nanjing University of Aeronautics and Astronautics, Nanjing, 2007.